Statistical thermodynamics of a two-dimensional cellular system

J. R. Iglesias and Rita M. C. de Almeida
Instituto de Física, Universidade Federal do Rio Grande do Sul, Caixa Postal 15051, 91500 Porto Alegre, Rio Grande do Sul, Brazil
(Received 16 April 1990)

The principles of statistical physics are applied to the study of cellular systems. Cells that fill a flat surface are characterized by area, perimeter, and number of sides. A set of constraints is established, taking into account the main features of the structure, from both geometrical and physical points of view. The distribution functions of number of sides and area are calculated as well as the thermodynamic parameters. The results are in agreement with available experimental and computational data.

I. INTRODUCTION

Cellular systems are macroscopic or microscopic arrays of cells that fill space. Examples in two dimensions are soap froths,[1-6] sections of metallurgical aggregates,[7-9] and biological tissues.[10-12] These systems present common features that arise mainly from the geometry and topology of space filling,[13] but they differ in time evolution, which exhibits characteristics that are not yet fully determined.

Two-dimensional soap froths can be constructed in such a way that initially the bubbles are small and almost all six-sided and the structure is fairly ordered.[2] As time goes by, both the average size and the disorder increase.[2,4] However, recent experiments on soap froths[3] seem to indicate a final stable value for the second moment μ_2 of the distribution in number of sides W_n, of the order of 1.5. Also, in the case of normal grain growth in polycrystals this self-similar state happens for a typical value of $\mu_2 \cong 2.4$.[14] Numerical studies play an important role in describing structure evolution and several works have been performed, such as computer simulations of the Potts model by Anderson and co-workers,[15,16] soap simulation by Weaire and co-workers,[17-19] and recent numerical studies by Beenakker.[20]

One should bear in mind that soap-froth evolution and normal grain growth in polycrystals have common features but are not identical. Soap bubble walls can adjust themselves almost instantaneously to reduce interface energy, and hence the evolution can be considered as a succession of quasiequilibrium states. Polycrystals are generally further from equilibrium than soap froths and the boundary energy may depend on other factors, such as the relative orientation of the microcrystals; also the existence of pores (stable three-sided cells in soap froths) and impurities may be an additional complication.

Several authors have applied with relative success the methods of statistical physics (for a review see Ref. 14) and particularly the maximum entropy formalism[13,21,22] to describe the equilibrium states and the evolution of these systems. In a previous paper we have presented a derivation of the statistical mechanics of cellular systems by considering an appropriate phase space[23] and more recently we have obtained results that are in good agreement with experiments, but that introduce constraints not fully justified.[24]

Here we present the development of the statistical mechanics of an ideal two-dimensional (2D) cellular structure and concentrate on the study of a soap froth, paying special attention to the distribution of number of sides W_n and of area $\phi(a)$. In Sec. II we discuss the application of maximum entropy formalism and of the methods of statistical mechanics to this problem; in Sec. III we deduce from the physics of the system a set of constraints with a minimum number of *a priori* statements. In the subsequent sections (Secs. IV–VI) the distribution functions and thermodynamics variables are calculated and, whenever possible, a comparison with experimental and computational results is made.

II. STATEMENT OF THE PROBLEM

In the past decades the methods of statistical mechanics (SM) have been applied to study problems from neural networks[25] and powders,[26] to self-organization and the "big bang theory," showing the strength and generality of the formalism. Particularly, cellular systems in two dimensions have been studied from the point of view of maximum entropy formalism of statistical mechanics[27] by several authors.[13,21-24]

A large number of systems, an ensemble, can be constructed with identical macroscopic conditions, the dynamics satisfying the principle of microreversibility;[21] i.e., as in a gas, cell transformations are reversible in microscopic scale, although the evolution of the system as a whole may be irreversible. However, while SM methods can be applied to these systems to obtain ensemble averages, that is, to calculate mean values of the interesting parameters over a large number of "replicas" of the system, time averages are more difficult to define. This is because in the case of soap froths the equilibrium may be unstable; although a self-similar state is attained in froths,[3] metallurgical grains,[7,8] and computer simulations.[17,18] It is also not clear whether the system is ergodic on a macroscopic scale, i.e., it may reach an equilibrium state, without exploring all the accessible states in the

phase space.

With these precautions, it is possible to define the phase space of the system. Obviously an ideal way should be to characterize the system by the position, length, and angle of every side of every cell. This description, although complete, is too cumbersome to handle. Instead, a convenient set of parameters that contains the essential information is then chosen:[23,24] position, perimeter, area, and number of sides of each cell.

The number of sides n is relevant from both geometrical and physical reasons,[13] and the size of the cells is measured by perimeter and area. (The relation between them gives the degree of "distortion" of the cell compared with a regular polygon.) Also, as the cells must fill space and the entropy should be extensive, the position of the cell is included through the coordinates of its center of mass (x,y). The generalized coordinates of the i cell can then be written as (n_i,p_i,a_i,x_i,y_i), such that we deal with a $5N$-dimensional phase space.

The probability of finding the system at a given point of the phase space is given by the density function[23]

$$\rho=\rho(n_1,\ldots,n_N;p_1,\ldots,p_N;a_1,\ldots,a_N;\mathbf{x}_1,\ldots,\mathbf{x}_N) , \quad (1)$$

which is normalized over the phase space.

As was stated before, the variables are not independent (perimeter, area, and number of sides, for example, are clearly related). The relation between the variables is defined by a minimum set of constraints that will be discussed in what follows.

III. CONSTRAINTS

In maximum entropy formalism, information about macroscopic variables is introduced through constraints. We separate two kinds of constraints, which we loosely call geometrical and physical constraints.

A. Geometrical constraints

Geometrical constraints are those that every 2D cellular structure must fulfill to pave a flat surface without pores or overlaps. These conditions are universal and independent of the physical nature of a particular structure. We list these constraints below.

1. The maximum area

There is a geometrical relation between the number of sides n, perimeter p, and area a of a convex planar figure with straight sides. It can be stated in two equivalent ways: a minimum possible perimeter for a polygon with fixed n, and a, or a maximum possible area for a polygon with given p and n. We have chosen the second one and the maximum area is

$$a_{\max}(n,p)=\frac{p^2}{4n}\cot\frac{\pi}{n} . \quad (2)$$

This constraint is nonholonomic and is taken into account through a cutoff in area integrals. The sum operator over the phase space is then defined as

$$\Xi=\sum_{N=0}^{\infty}\prod_{i=1}^{N}\left[\sum_{n_i=3}^{\infty}\int_0^{\infty}dp_i\int_0^{a_{\max}}da_i\int_A d\mathbf{x}_i\right] , \quad (3)$$

where A is the total area covered by the cells. The sum over N indicates that the total number of cells of the structure is variable; we are dealing with a kind of grand-canonical ensemble.

2. The expected number of cells $\langle N\rangle$ and average area $\langle a\rangle$

A given flat surface of area A can be filled with different numbers N of cells, depending on the average size of cells. The relation between the average number of cells $\langle N\rangle$ and the average area per cell $\langle a\rangle$ is obviously

$$\langle N\rangle=\Xi\rho N=\frac{A}{\langle a\rangle} , \quad (4)$$

where A is the total area. When periodic boundary conditions are considered A and N go to infinity but $\langle a\rangle$ remains finite.

3. Euler condition

The vertices of cellular structures in equilibrium are threefold.[1,13] In this case, the Euler condition states that in flat 2D cellular systems with an infinite number of convex cells the average number of sides of a cell is six. This constraint can be written as

$$\Xi\rho\sum_{j=1}^{N}n_j=6\langle N\rangle , \quad (5)$$

where $\langle N\rangle$ is the mean number of cells.

4. The average side length

There is a correlation between the number of sides of a cell and of its neighbors given by the almost universal, semiempirical Aboav-Weaire law.[4,13] This condition is due to the fact that every side is shared by two cells. This geometrical feature of the cellular system—being a connected array rather than a set of separate cells—generates a correlation between the number of sides and the perimeter. When no correlation is taken into account, the average perimeter of n-sided cells is independent of n.[23] As a consequence, the average side length of n-sided cells varies as n^{-1}; i.e., on the average, low-n-sided cells have longer sides, and high-n-sided cells, shorter ones. This is not observed, and also it is not possible to construct a homogeneous, connected array with such a set of cells. Here we take the simplest choice of a correlation between n and p that allows the array of cells to be connected: a constant average side length l.[24] This condition is written as

$$\Xi\rho\sum_{j=1}^{N}(p_j-n_jl)\delta_{n_jn}=0 . \quad (6)$$

Also, as stated by Rivier and collaborators,[13,21,22,28] a linear correlation between the random variables increases the entropy by reducing the number of linearly independent Lagrange multipliers.

One can consider Eq. (6) as a constraint that provides

the system with the information that only sets of cells that can be connected should be considered as possible microstates. Although in real systems l may depend on n, different assumptions regarding the average side length of n-sided cells would not increase the entropy.

B. Physical constraints

The physical constraints are the conditions that describe the dynamics of a cellular system. As these structures may be of very different nature, one cannot expect that physical constraints should be as general as geometrical ones. For the particular cases of soap froths and metallurgical aggregates, the energy is stored mainly in the interfaces of the cells and hence the total perimeter is minimized whenever possible. Also, very distorted cells, when compared with regular polygons, are very expensive in energy, because they have bigger perimeters for a given area. Finally, we consider just isothermal, mass-conserving transformations. Thermal energy of the total matter inside the cells (gas or solid) will remain constant and we shall not take it explicitly into account.

Assuming that the linear density of energy stored in the interfaces is constant, the perimeter energy of a cellular system is proportional to the total perimeter of the structure. While up to now only cells with straight sides and perimeter p have been considered, it is well known that soap-bubble walls present curvatures due to the difference of pressure in adjacent bubbles. Grain boundaries are also curved. This happens because threefold vertices are stable when the angles are 120°. Appendix A presents an estimate of the average correction in side lengths of n-sided cells due to the bending of the walls to match the 120° angles. It results in longer perimeters given by

$$p^*=p\frac{\theta_n}{\sin\theta_n} , \tag{7}$$

where p^* is the corrected perimeter and θ_n is

$$\theta_n=\frac{\pi(n-6)}{6n} . \tag{8}$$

As a function of the corrected p^* the interface energy term reads

$$E_p=\frac{\sigma}{2}\sum_{i=1}^{N}p_i\frac{\theta_{n_i}}{\sin\theta_{n_i}} , \tag{9}$$

and it differs from Eq. (8) of Ref. 23 just for the bending correction. The expression is exact for regular polygons and presents a very reasonable approximation for nonregular ones. One should observe that it gives a minimum of energy for $n=6$, as is expected.

Also, the area of a cell with n sides and perimeter p can vary from zero to a maximum value [the area of the regular polygon, Eq. (2)]. But flattened cells are too expensive in energy, i.e., distortion energy is lowest for a regular polygon and is very high when the area goes to zero.

An exact evaluation of this distortion energy depends on the particularities of the system, and may be difficult to handle. Taking into account the desired behavior—i.e., the energy must be minimum for the regular cell and go to large values for very distorted ones—we have chosen a particularly simple form of the distortion energy,

$$E_D=Cnl\ln\left[\frac{a_{\max}}{a}\right] , \tag{10}$$

that can be associated, in a crude estimate, to the isothermal work to compress a cell from the maximum area $a_{\max}$ to an area a:

$$W=-\int_{a_{\max}}^{a}\frac{NRT}{a'}da'=Pa\ln\left[\frac{a_{\max}}{a}\right] . \tag{11}$$

The constant C should be of the order of $P_c/nl\sim 0.1(\sigma/2)$. Equation (10) describes the cost in energy to smash a cell, and it is simple to deal with, but it is easily verified that the detailed form of the distortion energy is not crucial, provided it behaves as mentioned above.

The constraint associated to the total energy is then

$$\Xi\rho\sum_{i=1}^{N}\left[\frac{\sigma}{2}p_i\frac{\theta_{n_i}}{\sin\theta_{n_i}}+Cn_il\ln\left[\frac{a^i_{\max}}{a^i}\right]\right]=\langle E\rangle . \tag{12}$$

IV. MAXIMUM ENTROPY FORMALISM

We define the entropy as[23,27]

$$S=-\Xi\rho\ln(\lambda^5N!\rho) , \tag{13}$$

where λ^5 is a unit volume in the phase space equivalent to the constant h defined in SM textbooks,[29] $N!$ is introduced to correctly count the number of microstates, and ρ is the density function defined in Eq. (1).

To maximize the entropy subjected to the constraints, Eqs. (3)–(6) and (12), one defines the function Ψ, the generalized entropy,

$$\Psi=S-\alpha_1\Xi\rho-\alpha_2\Xi\rho\sum_{j=1}^{N}\left[\frac{\sigma}{2}p_j\frac{\theta_{n_j}}{\sin\theta_{n_j}}+Cn_jl\ln\left[\frac{a^j_{\max}}{a^j}\right]\right]-\alpha_4\Xi\rho\sum_{j=1}^{N}n_j-\alpha_5\Xi\rho N-\sum_{n=3}^{\infty}\alpha_6(n)\Xi\rho\sum_{j=1}^{N}(p_j-nl)\delta_{n_jn} , \tag{14}$$

where the α_i's are Lagrange multipliers.

By maximizing Ψ we obtain the density function ρ:[23]

$$\rho=\frac{1}{Z\lambda^{5N}N!}\exp\left\{-\alpha_5 N-\alpha_4\sum_{j=1}^{N}n_j-\sum_{j=1}^{N}\alpha_6(n_j)(p_j-n_j l)-\alpha_2\sum_{j=1}^{N}\left[\frac{\sigma}{2}p_j\frac{\theta_{n_j}}{\sin\theta_{n_j}}+Cn_j l\ln\left[\frac{a_{\max}^{j}}{a^{j}}\right]\right]\right\}, \tag{15}$$

where Z is the partition function and reads

$$Z=\Xi\frac{1}{\lambda^{5N}N!}\exp\left\{-\alpha_5 N-\alpha_4\sum_{j=1}^{N}n_j-\sum_{j=1}^{N}\alpha_6(n_j)(p_j-n_j l)-\alpha_2\sum_{j=1}^{N}\left[\frac{\sigma}{2}p_j\frac{\theta_{n_j}}{\sin\theta_{n_j}}+Cn_j l\ln\left[\frac{a_{\max}^{j}}{a^{j}}\right]\right]\right\}. \tag{16}$$

Lagrange multipliers here do not have an immediate physical meaning. They are determined through the constraint equations and the density function ρ. The generalized entropy Ψ is a kind of thermodynamic potential, such as the free energy. In that sense, the introduction of a free energy and a temperature in Refs. 23 and 24 was rather misleading. However, an order disorder transition[24] still happens, but as a function of α_2. While α_5 is related to the chemical potential, α_2 is associated with a generalized temperature. In fact, α_2 is a measure of the average perimeter and distortion energy per cell and it is not the usual temperature because it does not control heat flux. The role of α_2 is to control energy flux between two cellular systems at the same temperature in contact with each other.

V. PARTITION FUNCTION AND THERMODYNAMICAL POTENTIAL

The thermodynamical variables and the distribution functions can be derived from the density function ρ and the partition function Z. In what follows, we calculate Z, the Lagrange multipliers, and the distribution functions.

A. Partition function

Using Eq. (16), the partition function can be written as

$$Z=\sum_{N=0}^{\infty}\frac{e^{-\alpha_5 N}A^{N}Q^{N}}{\lambda^{5N}N!}=\exp\left[\frac{e^{-\alpha_5}AQ}{\lambda^{5}}\right], \tag{17}$$

where

$$Q=\sum_{n=3}^{\infty}e^{-\alpha_4 n-\alpha_6(n)nl}\int_0^{\infty}dp\,e^{-\alpha_2(\sigma/2)p(\theta_n/\sin\theta_n)-\alpha_6(n)p}\int_0^{a_{\max}}e^{\alpha_2 nlC\ln(a/a_{\max})}. \tag{18}$$

The area integrals converge if and only if $\alpha_2 nlC>-1$. Then, as there is not an upper limit for l and n, and both are positive, it must be

$$\alpha_2 C>0\ . \tag{19}$$

Also, by means of Eqs. (4), (17), and (18), one arrives at

$$\alpha_6(n)=\frac{3}{nl}-\alpha_2\frac{\sigma}{2}\frac{\theta_n}{\sin\theta_n} \tag{20}$$

and Q reduces to

$$Q=\frac{2e^{3}l^{3}}{27}\sum_{n=3}^{\infty}\frac{e^{-\alpha_4 n-\alpha_2(\sigma/2)nl(\theta_n/\sin\theta_n)}n^{3}k_n}{\alpha_2 Cnl+1}, \tag{21}$$

where

$$k_n=\frac{1}{4n}\cot\left[\frac{\pi}{n}\right] \tag{22}$$

and θ_n is given by Eq. (8).

The Lagrange multiplier α_5 is determined as a function of α_2 and α_4:

$$\alpha_5=3+\ln\left[\frac{8l^{5}}{81\lambda^{5}}\sum_{n=3}^{\infty}\frac{e^{-\alpha_4 n-\alpha_2(\sigma/2)nl(\theta_n/\sin\theta_n)}k_n^{2}n^{5}}{\alpha_2 Cnl+2}\right], \tag{23}$$

and finally, α_2 and α_4 are found by numerically solving Eqs. (4) and (12), which are rewritten as

$$-\frac{1}{Q}\frac{\partial Q}{\partial\alpha_2}=\frac{\langle E\rangle}{\langle N\rangle}, \tag{24a}$$

$$-\frac{1}{Q}\frac{\partial Q}{\partial\alpha_4}=6\langle N\rangle\ . \tag{24b}$$

Formally, the problem is solved: through Eqs. (24), the values of α_2 and α_4 are numerically obtained, as a function of $\langle N\rangle$ and $\langle E\rangle$, and from Eq. (23) α_5 is determined. The partition function can then be calculated, as well as other thermodynamic variables, as shown in the following.

B. Distribution functions

We present the distribution functions related to the random variables n, p, and a. These distribution functions explain the role of the Lagrange multipliers α_2 and α_4 as well as the character of the differences related to configurations with different α_2 of the cellular system.

1. Reduced probability distribution $f(n,p,a)$

The reduced probability distribution $f(n,p,a)$ is the probability of finding a cell with n sides, perimeter p and

area a in an equilibrium configuration of the cellular system. It is

$$f(n,p,a)=\frac{1}{Q}\left[\frac{a}{a_{\max}}\right]^{\alpha_2 Cnl} \times\exp\left[-\alpha_4 n-\alpha_2\frac{\sigma}{2}nl\frac{\theta_n}{\sin\theta_n}-\frac{3p}{nl}\right] \quad (25)$$

for $a\le a_{\max}$ and zero otherwise.

In Eq. (25) Q is the reduced partition function defined in Eq. (21) and $a_{\max}$ is given by Eq. (2). As far as we know, this function has not been measured for any natural system, but is very useful in obtaining other distribution functions and thermodynamic quantities that can be compared with experiments and numerical simulations.

2. *Relative number of n-sided cells, W_n*

The relative number of n-sided cells, W_n, can easily be obtained from Eq. (25) by integrating over area and perimeter:

$$W_n=\frac{1}{S_1}\frac{n^3k_n\exp\left[-\alpha_4 n-\alpha_2\frac{\sigma}{2}nl\frac{\theta_n}{\sin\theta_n}\right]}{\alpha_2 Cnl+1}, \quad (26)$$

where

$$S_1=\sum_{n=3}^{\infty}\frac{n^3k_n\exp\left[-\alpha_4 n-\alpha_2\frac{\sigma}{2}nl\frac{\theta_n}{\sin\theta_n}\right]}{\alpha_2 Cnl+1} \quad (27)$$

is the normalization factor and k_n is given by Eq. (22).

A relevant quantity is the second moment μ_2 of W_n, which measures the dispersion of n around the average value $\langle n\rangle=6$. It is calculated as

$$\mu_2=\sum_{n=3}^{\infty}(n-6)^2W_n , \quad (28)$$

and is univocally connected to the values of α_2, which are associated with the energy of the system: there is a one-to-one relation between the topological disorder μ_2 and the energy of the froth. We shall come back to this point later.

Figure (1) shows plots of W_n versus n [Eq. (26)] and a comparison with experimental results for soap froths by Aboav[4] and by Stavans and Glazier.[3] The theoretical and experimental results show the same qualitative behavior and are in good agreement for four different values of μ_2, including the long-term self-similar state proposed in Ref. 3.

For $\alpha_2=0$ the topological disorder is maximum at $\mu_2=5.98$, a result obtained in previous calculations.[24] This maximum value depends on the assumption of the average side-length dependence on n [Eq. (6)], and on $\mu_2\to 0$ when $\alpha_2\to\infty$, as expected.

3. *Area distribution $\phi(a)$*

The area distribution $\phi(a)$ is defined from the reduced probability $f(n,p,a)$ as follows:

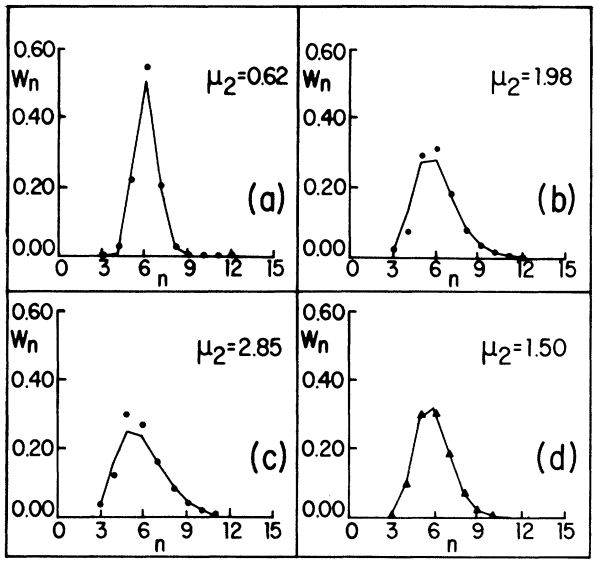

FIG. 1. Relative number of n-sided cells, W_n, as a function of n. The solid lines are the theoretical curves. The dots in (a)–(c) refer to experimental data for soap froths by Aboav (Refs. 4 and 5) and in (d) the triangles correspond to the experiments by Stavans and Glazier (Ref. 3) for a soap froth after an evolution time of 29.48 h. Observe the shift in the maximum of the distribution from $n=6$ to 5 as μ_2 increases, in both theory and experiments.

$$\phi(a)=\sum_{n=3}^{\infty}\int_0^{\infty}dp\int_0^{p^2k_n}da'\,\delta(a-a')f(n,p,a') . \quad (29)$$

Hence the average area of the cells is

$$\eta=\int_0^{\infty}da\,a\phi(a)=\frac{4l^2}{3}\frac{S_2}{S_1} , \quad (30)$$

where S_1 is given by Eq. (27) and S_2 is

$$S_2=\sum_{n=3}^{\infty}\frac{n^5k_n^2\exp\left[-\alpha_4 n-\alpha_2\frac{\sigma}{2}nl\frac{\theta_n}{\sin\theta_n}\right]}{(\alpha_2 Cnl+2)} . \quad (31)$$

A plot of $\langle a\rangle$ versus μ_2 is presented in Fig. 2. The average area is fairly constant for $\mu_2\le 4$ and decreases when μ_2 approaches its maximum value 5.98. When $\langle a\rangle$ decreases, the total number of cells and the total perimeter increase, i.e., the energy of interface increases.

Figure 3 shows $\phi(a/\langle a\rangle)$ versus $a/\langle a\rangle$. This distribution is obtained by numerically performing first the perimeter integral and then summing from $n=3$ to 25 for the same values of μ_2 of Fig. 1 (dashed lines). The solid line stands for the experimental data by Glazier *et al.*[30] for a froth with an evolution time of 3163 min and $\mu_2\approx 1.5$ that corresponds, according to the authors, to the self-similar state. Earlier area distributions show maxima that shift towards lower values of $a/\langle a\rangle$. The maxima in the theoretical curves are roughly at the same position because they correspond to the maximum entropy ("equilibrium") state; however, the height of the peaks

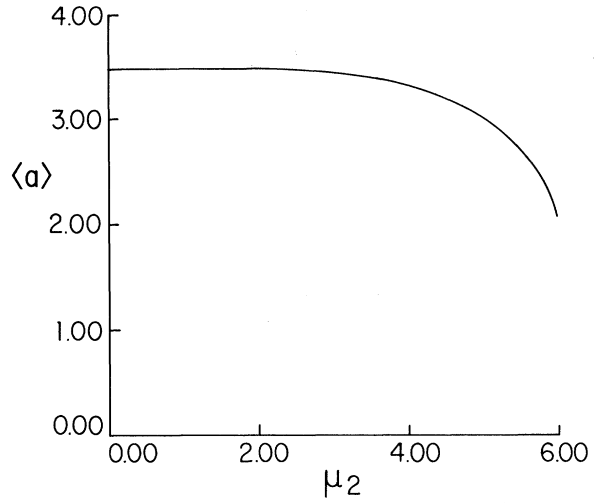

FIG. 2. Average area $\langle a \rangle$, in units of l^2 vs the topological disorder μ_2. $\langle a \rangle$ decreases if $\mu_2 \geq 3.0$, increasing the mean number of cells $\langle N \rangle$ and also the perimeter energy per area.

decreases when μ_2 decreases because the probability of finding more regular cells with higher values of $a/\langle a \rangle$ increases. In the experimental steady state the average area is continuously growing but the distribution functions are self-similar. In the present formulation this can be described by allowing the average length l to increase in time: the theoretical distribution $\phi(a/\langle a \rangle)$ remains constant, in agreement with the experiments. In this sense the self-similar state can be compared to the theoretical equilibrium (maximum entropy) state. Finally, the experimental data regarding area distributions are much less reliable than other measured quantities,[31] and also the value of C in Eq. (11), which plays an important role in the behavior of $\phi(a/\langle a \rangle)$, is only a rough estimate, as can be seen in Appendix B. Taking these facts into account, the results are in excellent agreement with experiments.

C. The average area of n-sided cells $\langle a_n \rangle$

The average area of n-sided cells is easily obtained from the reduced probability distribution

$$\langle a_n \rangle = \sum_{n'=3}^{\infty} \int_0^{\infty} dp \int_0^{a_{\max}} da\, f(n',p,a) a \delta_{n,n'}$$

$$= \tfrac{4}{3} l^2 \frac{\alpha_2 C n l + 1}{\alpha_2 C n l + 2} k_n n^2 . \tag{32}$$

Equation (32) is plotted in Fig. 4; it is clear that there is not a significant dependence of $\langle a_n \rangle$ on the value of α_2. Figure 4 shows a good agreement of the theoretical curves with the experimental results by Glazier, Gross, and Stavans.[2]

Lewis's hypothesis[32] states that $\langle a_n \rangle = A + B_n$, where A and B are undetermined constants. Clearly, Eq. (32) is not a linear relation. Nevertheless, for low topological disorder (values of $\mu_2 \leq 3.0$), the structure shows mainly bubbles with $3 \leq n \leq 12$. In this region, the error bars of experimental results do not allow one to decide between Lewis's hypothesis or Eq. (32). Also, the fraction $\langle a_6 \rangle / \langle a \rangle = 1$, which has been suggested as a test for Lewis's relation,[33] when calculated through Eq. (32), varies in the range $0.9 \geq \langle a_6 \rangle / \langle a \rangle < 1$. We conclude that it is very difficult to decide between Lewis's law and Eq. (32) from experimental data: they are approximately equal for values of $\mu_2 \leq 3.0$.

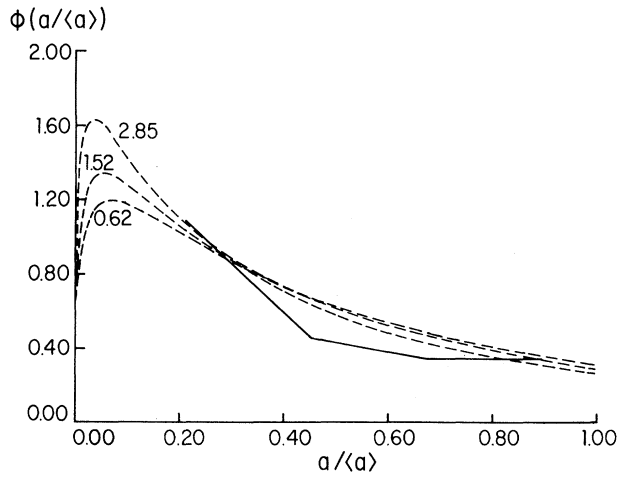

FIG. 3. Relative area distribution $\phi(a/\langle a \rangle)$ vs $a/\langle a \rangle$. The dashed lines are theoretical curves for different values of μ_2 and the solid line refers to the experimental data by Glazier *et al.* (Ref. 30) for an evolution time of 3163 min and $\mu_2 \approx 1.5$.

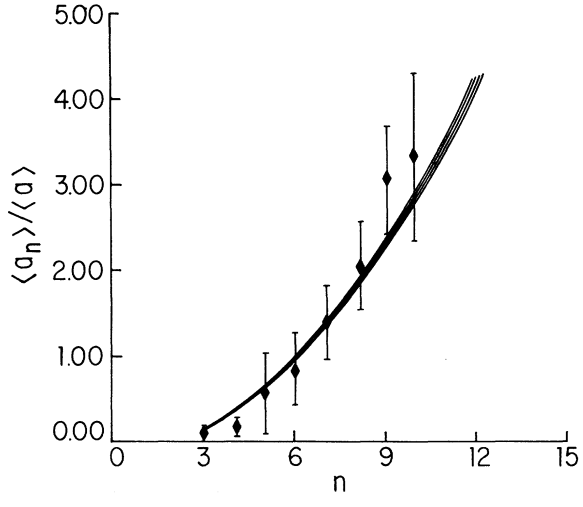

FIG. 4. Normalized averages of n-sided cells vs n. The solid lines correspond to theoretical calculations with different values of μ_2 (from 0.62 to 2.85). The points and error bars are the experimental data for soap froths by Glazier, Gross and Stavans (Ref. 2).

D. Energy

Using the density function we calculate the average energy per cell:

$$\frac{\langle E\rangle}{\langle N\rangle}=Cl\left\langle\frac{n}{\alpha_2 Cnl+1}\right\rangle+\frac{\sigma}{2}l\left\langle n\frac{\theta_n}{\sin\theta_n}\right\rangle . \tag{33}$$

The first and second terms in Eq. (33) are, respectively, the average distortion and perimeter energy per cell. We have plotted separately these terms as well as $\langle E\rangle/\langle N\rangle$ as functions of the topological disorder μ_2 for $C=0.1(\sigma/2)$ in Fig. 5. The average perimeter energy per cell is fairly constant, due to the imposed constant average side length and to the Euler condition $\langle n\rangle=6$, since $\theta_n/\sin\theta_n$ does not vary considerably for $3\leq n\leq\infty$. Distortion energy increases with μ_2. Although it is much less than the perimeter energy (see Fig. 5) it is essential in preventing zero area cells to appear in the froth; although, as stated before, its exact form seems not to be important.

When considering the froth as a whole, the relevant quantity is the energy per area that is plotted in Fig. 6. Again, we present perimeter and distortion energy terms separately as functions of μ_2. Perimeter energy per area increases with μ_2 because the average area $\langle a\rangle$ decreases with topological disorder, as is shown on Fig. 2. The total energy per area increases with μ_2 and has a fairly flat behavior for $1\leq\mu_2\leq 3.0$, which is in qualitative agreement with the experimental fact that μ_2 stops increasing at $\mu_2\approx 1.5$.[3]

Distortion energy has a twofold effect on the behavior of the total energy per area: (i) it has an average value that increases with μ_2, and (ii) it modifies the reduced distribution function, Eq. (25), preventing zero area cells to appear. When this energy term is not considered, $\langle a\rangle$ increases with μ_2.[24] Hence the increase of the average perimeter energy with topological disorder is also an effect of the distortion energy term. One remarks that μ_2 is not a free parameter but is univocally determined by α_2, which, in its turn, is the Lagrange multiplier associated with the energy of the system. Then, the determination of μ_2 implies the fixing of the energy and vice versa. However, as μ_2 is a measurable quantity, it is the appropriate parameter to be chosen as the independent one.

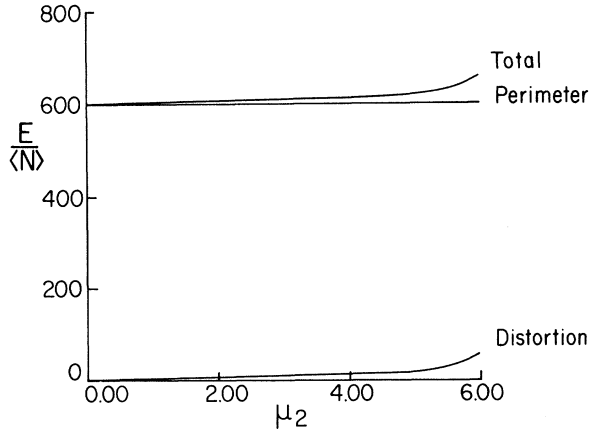

FIG. 5. Distortion, perimeter, and total energy per cell (in units of $\sigma/2l$) vs the topological disorder μ_2.

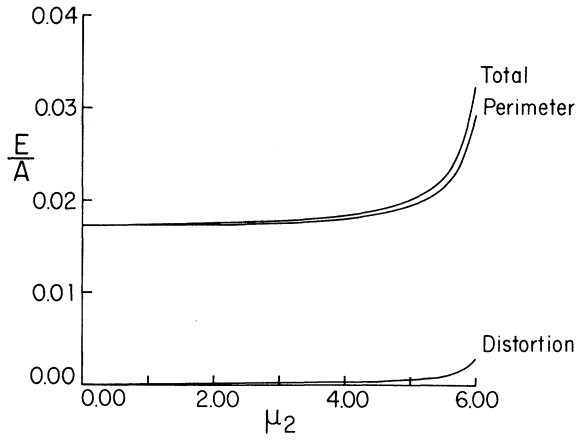

FIG. 6. Distortion, perimeter, and total energy per unit area (in units of $\sigma/2l$) vs the topological disorder μ_2.

VI. CONCLUSIONS

We have presented a theoretical model to describe the equilibrium configurations of cellular systems, particularly soap froths, by means of the methods of SM through the maximum entropy principle. The generalized entropy has been calculated, including a minimum set of constraints. The geometrical constraints are the "natural" ones, but the average side length l is introduced as the simplest hypothesis, after verifying that a structure with no correlation between p and n violates Aboav and Weaire's law. On the other hand, no explicit constraint on the disorder μ_2 is imposed except through the total energy, improving the model and results of Ref. 24. The energy terms include interface energy, bending of the sides, and cell distortion. These contributions are particularly adequate to describe soap froths but one can easily generalize the model to other cellular systems such as metallurgical aggregates.

As in Ref. 24 we have obtained a remarkable agreement with experimental results for the cells distribution of the number of sides and the mean value of the area of n-sided cells as functions of n. We obtain a theoretical equation different from Lewis's law,[32] but in the region $0\leq\mu_2\leq 3.0$ both expressions and experiments[4] yield to similar numerical results. It would be interesting to investigate systems with greater disorder, like those described by Fortes and Andrade.[34]

Finally, the area distribution $\phi(a/\langle a\rangle)$ is calculated for the first time within this method, and it is in good agreement with the results of Glazier and co-workers.[30,31] We remark that the taking into account of distortion energy is essential for arriving at reasonable results. Otherwise, nothing prevents zero area cells, and $\phi(a/\langle a\rangle)$ presents a maximum for $a\rightarrow 0$.

From these considerations we conclude that SM methods are well suited to describe cellular systems, mainly soap froths. An appropriate choice of energy will enable us to describe other cellular systems.

ACKNOWLEDGMENTS

We acknowledge discussions with Professor E. V. Anda, Professor M. A. Gusmão, Professor M. E. Foglio, and correspondence with Dr. N. Rivier. Financial support from the Brazilian agencies, Conselho Nacional de Desenvolvimento Científico e Tecnológico (CNPq), Financiadora de Estudos e Projetos (FINEP), and Fundação de Amparo à Pesquisa do Estado do Rio Grande do Sul (FAPERGS), is also acknowledged.

APPENDIX A

A regular polygon of n sides of length l has an internal angle given by

$$\beta_n = \frac{\pi(n-2)}{n} . \tag{A1}$$

When its sides bend to make angles of $2\pi/3$ they deviate from the straight-line position by an angle θ_n given by

$$\theta_n = \frac{1}{2}\left[\beta_n - \frac{2\pi}{3}\right] = \frac{\pi}{6n}(n-6) , \tag{A2}$$

and a bent side l^* can be considered as an arc of circumference that measures $2\theta_n$ with radius $R = l/2\sin\theta_n$. The length of the arc l^* is

$$l^* = \frac{l\theta_n}{\sin\theta_n} , \tag{A3}$$

and the corrected perimeter p^* of the polygon reads

$$p^* = \frac{nl\theta_n}{\sin\theta_n} = p\frac{\theta_n}{\sin\theta_n} . \tag{A4}$$

APPENDIX B

In a soap froth the difference of pressure between two adjacent bubbles causes a curvature on the common wall. Surface tension of the soap film acts to restore the walls to the straight-line position. Equilibrium is attained when internal pressure and surface tension compensate each other.

Surface tension can be deduced from perimeter energy:

$$\frac{\partial E_p}{\partial p} = \frac{\sigma}{2} , \tag{B1}$$

where E_p is the perimeter energy.

The force per unit length due to surface tension is $\sigma/2nl$, and it must be equal to internal pressure (assuming an ideal gas). Hence

$$Pa = \frac{\sigma}{2nl}a . \tag{B2}$$

Taking the value of the average area of n-sided cells, Eq. (32), and comparing Eqs. (10) and (11), we estimate the order of C as

$$C \approx 0.1\frac{\sigma}{2} . \tag{B3}$$

[1] C. S. Smith, *Metal Interfaces* (American Society for Metals, Metals Park, OH, 1952), p. 65.
[2] J. A. Glazier, S. P. Gross, and J. Stavans, Phys. Rev. A **36**, 306 (1987).
[3] J. Stavans and J. A. Glazier, Phys. Rev. Lett. **62**, 1318 (1989).
[4] D. A. Aboav, Metallography **13**, 43 (1980).
[5] D. A. Aboav, Metallography **16**, 265 (1983).
[6] D. A. Aboav, Metallography **17**, 383 (1984).
[7] D. A. Aboav and T. G. Langdon, Metallography **2**, 171 (1969).
[8] P. A. Beck, Adv. Phys. **3**, 245 (1954).
[9] H. E. Exner, Int. Metall. Rev. **17**, 25 (1972).
[10] H. J. Honda, J. Theor. Biol. **32**, 523 (1978).
[11] V. V. Smoljaninov, *Mathematical Models of Biological Tissues* (Nauka, Moscow 1980), in Russian.
[12] J. C. M. Mombach, M. A. Z. Vasconcellos, and R. M. C. de Almeida, J. Phys. D **23**, 600 (1990).
[13] D. Weaire and N. Rivier, Contemp. Phys. **25**, 59 (1984).
[14] H. V. Atkinsons, Acta Metall. **36**, 469 (1988).
[15] M. P. Anderson, D. J. Srolovitz, G. S. Grest, and P. S. Sahni, Acta Metall. **32**, 783 (1984).
[16] D. J. Srolovitz, M. P. Anderson, P. S. Sahni, and G. S. Grest, Acta. Metall. **32**, 793 (1984).
[17] D. Weaire and J. P. Kermode, Philos. Mag. B **48**, 245 (1983).
[18] D. Weaire and J. P. Kermode, Philos. Mag. B **50**, 379 (1984).
[19] J. Wejchert, D. Weaire, and J. P. Kermode, Philos. Mag. B **53**, 15 (1986).
[20] C. W. J. Beenakker, Phys. Rev. A **37**, 1697 (1988).
[21] N. Rivier, Philos. Mag. B **52**, 795 (1985).
[22] N. Rivier, Physica D **23**, 129 (1986).
[23] R. M. C. de Almeida and J. R. Iglesias, J. Phys. A **21**, 3365 (1988).
[24] R. M. C. de Almeida and J. R. Iglesias, Phys. Lett. A **138**, 253 (1989).
[25] B. Lautrup (unpublished).
[26] S. F. Edwards and R. B. S. Oakeshott, Physica A **157**, 1080 (1989).
[27] E. T. Jaynes, Phys. Rev. **106**, 620 (1957).
[28] N. Rivier and A. Lissowski, J. Phys. A **15**, 2143 (1982).
[29] K. Huang, *Statistical Mechanics* (Wiley, New York, 1963).
[30] J. A. Glazier, M. P. Anderson, G. S. Grest, and J. Stavans (unpublished).
[31] J. Glazier, Ph.D. thesis, The University of Chicago, Chicago, 1989.
[32] F. T. Lewis, Anat. Rec. **38**, 341 (1928).
[33] N. Rivier, in *Maximum Entropy and Bayesian Methods*, edited by P. F. Fougere (Kluwer, Dordrecht, 1990), p. 297.
[34] M. A. Fortes and P. N. Andrade, J. Phys. (Paris) **50**, 717 (1989).